92. Hydrogenation of the *ansa*-Chain of Rifamycins. X-Ray Crystal Structure of (16*S*)-16,17,18,19-Tetrahydrorifamycin S

by **Cecilia Bartolucci, Luciano Cellai*, Silvio Cerrini, Patrizia Di Filippo, Doriano Lamba,** and **Anna Laura Segre**

Istituto di Strutturistica Chimica 'Giordano Giacomello', CNR, CP 10, I-00016 Monterotondo Stazione, Roma

and **Armando Doriano Bianco, Marcella Guiso,** and **Vinicio Pasquali**

Dipartimento di Chimica, Università 'La Sapienza', I-00185 Roma

and **Mario Brufani**

Dipartimento di Scienze Biochimiche, Università 'La Sapienza', I-00185 Roma

(15.II.93)

The catalytic hydrogenation of rifamycin S (**2**) over Pd/C, followed by oxidation with $K_3[Fe(CN)_6]$, generates a pair of 16,17,18,19-tetrahydrorifamycins S (**3**/**4**), epimeric at C(16). The use of PtO_2 as catalyst leads to the hydrogenation also of the C(28)=C(29) bond giving, after oxidation by $K_3[Fe(CN)_6]$, a mixture of the epimers (16*R*)- and (16*S*)-16,17,18,19,28,29-hexahydrorifamycins S (**5**/**6**). Furthermore, we synthesized the (16*R*)- and (16*S*)-3-bromo derivatives **7**/**8** and (16*R*)- and (16*S*)-3-(piperidin-1-yl) derivatives **9**/**10**. The determination of the X-ray crystal structure of the most abundant epimer **4** of the tetrahydrorifamycins allowed the assignment of the absolute configuration at C(16) of all derivatives. A structure-activity relationship study showed that in general the (16*R*)-epimers are more potent inhibitors of bacterial RNA polymerase than the (16*S*)-epimers.

Introduction. – Rifamycins are a well-known class of antibacterial antibiotics produced by a strain of *Nocardia mediterranei*. They are specific inhibitors of bacterial DNA-dependent RNA polymerase (DDRP) [1]. Among these compounds, the most studied are rifamycin SV (**1**; *Scheme 1*) and its quinone form rifamycin S (**2**). Rifamycin S

Scheme 1

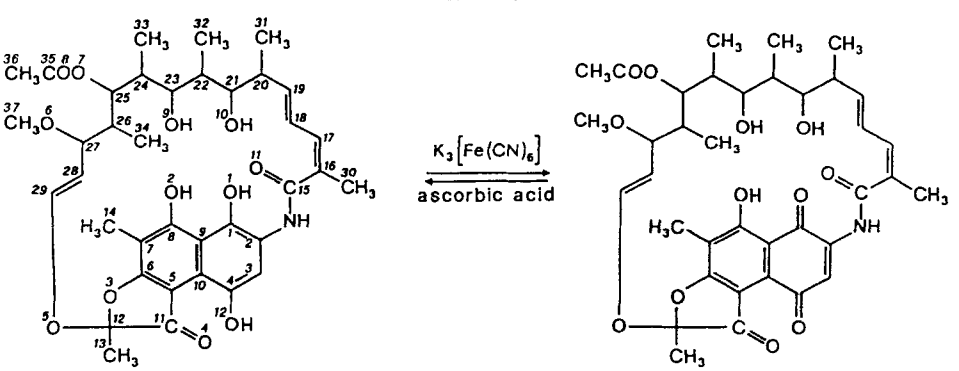

1 Rifamycin SV

2 Rifamycin S

was used both for the chemical-structure elucidation [2] and for the study of the chemical reactivity of this class of antibiotics [3] [4], and it was then used as starting compound for the preparation of hundreds of semisynthetic derivatives, aimed at the improvement of the pharmacological properties.

Rifamycin S consists of a seventeen-membered aliphatic *ansa*-chain, spanning two nonadjacent positions of a naphthoquinone system. The *ansa*-chain comprises two conjugated and one isolated double bond, usually referred to as C(16)=C(17)–C(18)=C(19) and C(28)=C(29), respectively. These double bonds can be partially or totally hydrogenated. The C(18)=C(19) bond can be selectively hydrogenated by the action of hydrazine [5], while a 16,17-dihydro derivative was obtained by fermentation [6]. By hydrogenation in the presence of Pd/C, one obtains 16,17,18,19-tetrahydrorifamycin S, while the use of PtO_2 as catalyst leads to 16,17,18,19,28,29-hexahydrorifamycin S [3], in both cases after reoxidation to the quinone form with $K_3[Fe(CN)_6]$ (see below, *Scheme 2*).

Since C(16) of rifamycins is a prochiral centre, the hydrogenation of the C(16)=C(17) bond yields pair of diastereoisomers. This fact was known [2], but it was never taken into consideration, and the derivatives containing hydrogenated C(16)=C(17) were always mentioned without specifying the chirality at C(16).

This paper reports the synthesis and isolation of the (16*R*)- and (16*S*)-epimers of tetrahydro-, hexahydro-, 3-bromo-tetrahydro-, and tetrahydro-3-(piperidin-1-yl)-rifamycin S. The determination of the X-ray crystal structure of the most abundant epimer **4** of the tetrahydrorifamycins S allowed the assignment of the absolute configuration at C(16) in all above compounds.

Since the hydrogenation of the double bonds affects the activity of rifamycins [7], we tested these compounds as inhibitors of DDRP from both a wild and a *Rif*-resistant bacterial strain.

Synthesis. – The tetrahydrorifamycin S epimers **3**/**4** and hexahydrorifamycin S epimers **5**/**6** were synthesized by hydrogenation over Pd/C and over PtO_2, respectively, and oxidation by $K_3[Fe(CN)_6]$, as previously described [2] [3] (*Scheme 2*). In both cases, the epimers were only separable in the hydroquinone-SV form, and not in the quinone-S form. The separations were achieved by column chromatography (CC; silica gel). On hydrogenation over PtO_2, the fastest eluting tetrahydro epimer **4** forms the fastest eluting hexahydro epimer **6** (*Scheme 2*). Similarly **5** was formed from **3**.

The 3-bromorifamycin SV was synthesized as described in [8] and hydrogenated over Rh/Al_2O_3 leading, after oxidation with $K_3[Fe(CN)_6]$, to a mixture of the (16*R*)- and (16*S*)-epimers **7** and **8**, respectively (*Scheme 3*), separable by CC. The hydroquinone form of **3** and **4**, obtained by reduction of **3** and **4** with ascorbic acid [2], led by bromination [8] to **7** and **8**, respectively.

The 3-(piperidin-1-yl)rifamycin S was synthesized as described in [4] and hydrogenated over Pd/C to give, after oxidation with MnO_2, a mixture of the (16*R*)- and (16*S*)-epimers **9** and **10**, respectively (*Scheme 3*), separable by CC. The reaction of **3** and **4** with piperidine, carried out as described in [4], led to the same **9** and **10**, respectively.

The separation of **7** from **8** and of **9** from **10** was possible with the quinone forms, and differently from all other cases, the (16*R*)-epimer **7** was eluted before the (16*S*)-epimer **8**. The ^1H- and ^{13}C-NMR data for compounds **3**–**10** are reported in *Tables 1–3*.

Scheme 2

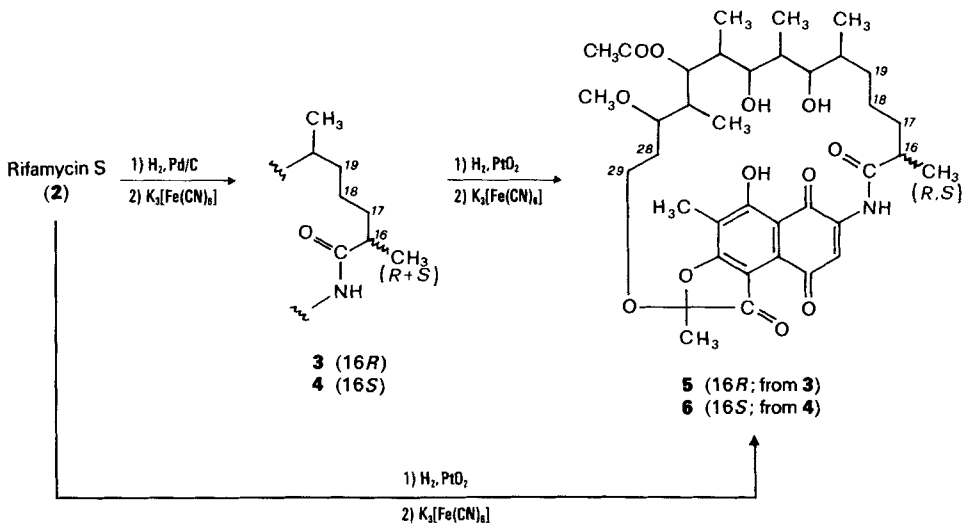

Scheme 3

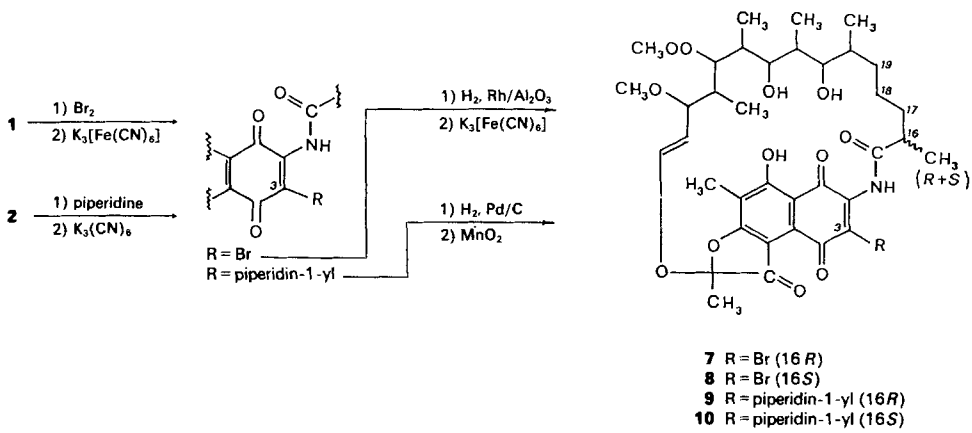

Table 1. *^{1}H-NMR Chemical Shifts* (in ppm rel. to Me_4Si; 600 MHz, $CDCl_3$) *for* **3**–**6**

	3	**4**	**5**	**6**
HN–C(15)	8.37	8.31	8.42	8.35
H–C(16)	2.62	2.60	2.63	2.60
CH_2(17)	1.18, 1.83	1.50, 1.68	1.82 (2 H)	1.28, 1.45
CH_2(18)	1.15, 1.37	1.15, 1.30	1.50 (2 H)	1.50, 1.73
CH_2(19)	1.32, 1.80	1.32, 1.65	1.34 (2 H)	1.30, 1.42
H–C(20)	1.84	1.70	1.68	1.53
H–C(21)	3.35	3.41	3.32	3.27

Table 1 (cont.)

	3	4	5	6
H–C(22)	1.80	1.72	1.70	1.63
H–C(23)	2.93	2.98	2.89	2.94
H–C(24)	1.49	1.65	1.48	1.50
H–C(25)	4.53	4.94	4.52	4.80
H–C(26)	1.90	1.60	1.99	1.81
H–C(27)	3.32	3.45	2.82	3.01
H–C(28) or CH_2(28)	4.33	5.08	1.35, 1.51	1.49, 1.70
H–C(29) or CH_2(29)	6.20	6.29	3.65 (2 H)	3.58 (2 H)
Me(30)	1.20	1.32	1.21	1.32
Me(31)	0.73	0.72	0.74	0.69
Me(32)	0.97	0.98	0.98	0.95
Me(33)	0.59	0.60	0.58	0.56
Me(34)	0.16	0.03	0.27	0.23
$MeCO_2$–C(25)	2.01	2.06	2.00	2.02
Me(37)	3.09	3.09	3.18	3.17
Me(13)	1.71	1.74	1.66	1.64
Me(14)	2.33	2.30	2.31	2.28
H–C(3)	7.86	7.83	7.84	7.84
OH–C(8)	12.58	12.56	12.57	12.52

Table 2. *^{13}C-NMR Chemical Shifts* (in ppm rel. to Me_4Si; 150 MHz, $CDCl_3$) *for Proton-Bearing C-Atoms of* **3**–**6**

	3	4	5	6
CH(3)	117.61	117.3	117.57	117.2
Me(13)	22.19	21.41	22.57	21.64
Me(14)	7.61	7.60	7.54	7.51
CH(16)	41.89	45.0	41.82	45.0
CH_2(17)	30.54	35.7	35.24	32.1
CH_2(18)	20.21	21.16	20.77	22.28
CH_2(19)	35.31	31.41	30.58	35.2
CH(20)	34.46	34.6	32.92	35.0
CH(21)	71.65	71.4	72.05	72.8
CH(22)	32.95	33.1	34.61	33.1
CH(23)	77.54	77.5	77.36	79.2
CH(24)	37.35	37.0	37.45	37.2
CH(25)	73.67	74.2	73.68	73.9
CH(26)	37.58	38.3	34.30	35.6
CH(27)	81.25	78.1	81.24	77.3
CH(28) or CH_2(28)	114.32	118.2	30.38	30.3
CH(29) or CH_2(29)	145.03	141.86	64.95	63.5
Me(30)	17.94	17.99	18.06	18.08
Me(31)	15.48	14.86	15.44	15.02
Me(32)	11.54	11.14	11.68	11.26
Me(33)	8.76	8.73	8.80	8.89
Me(34)	11.54	9.47	12.51	10.99
MeCO_2–C(25)	20.95	20.85	20.96	20.91
Me(37)	56.79	57.6	56.85	57.1

Table 3. *^{1}H-NMR Chemical Shifts* (in ppm rel. to Me_4Si; 300 MHz) *in $CDCl_3$ for* **7–10**[a])

	7	**8**	**9**	**10**
HN–C(15)	8.38	7.39	7.50	7.35
H–C(16)	2.66	2.50	2.55	2.50
H–C(21)	3.42	3.47	3.45	3.43
H–C(23)	2.91	2.96	2.93	2.95
H–C(25)	4.54	4.97	4.83	4.85
H–C(27)	3.30	3.39	3.31	3.28
H–C(28)	4.85	5.09	5.15	5.22
H–C(29)	6.12	6.08	6.14	6.16
Me(30)	1.21	1.31	1.20	1.31
Me(31)	0.74	0.71	0.75	0.72
Me(32)	0.96	0.96	0.97	0.98
Me(33)	0.60	0.59	0.57	0.57
Me(34)	0.16	0.07	0.28	0.15
$MeCO_2$–C(25)	1.99	2.05	2.01	2.01
Me(37)	3.07	3.07	3.09	3.07
Me(13)	1.72	1.72	1.69	1.68
Me(14)	2.31	2.28	2.25	2.26
OH–C(8)	12.65	12.29	13.50	13.40

[a]) The protons bound to C(17) to C(20), C(22), C(24), and C(26) of all four compounds **7–10** absorb in the range 1.1–1.9 ppm.

X-Ray Crystal Structure of 4. – The configuration at C(16) of **4** proved to be (*S*), on the basis of the known configuration of the chiral centers in **2** [9]. A perspective view of the molecular structure of **4** is shown in *Fig. 1*. Although the bonds C(21)–O(10) and C(23)–O(9) are parallel to the planar part of the molecule, the spatial arrangement of the four atoms O(1), O(2), O(9), and O(10), which is an important factor in the binding of rifamycins to DDRP [1] [10], differs in **4** from that found in rifamycin S [11] (**2**; *Table 4*). This is expected because of the hydrogenation at C(16) to C(19). *Fig. 2* shows the comparison of the conformation of **4** (full line) and **2** (dashed line), the weighted r.m.s. deviation being 0.53 Å. The best plane through the 17 atoms of the skeleton of the *ansa*-chain in **4** displays an angle of 95.2(3)° with the plane of the chromophore. The corresponding angle for **2** is 114.3(1)°. The amide group HN(1)–C(15)–O(11) is approximately coplanar with the naphthoquinone nucleus, the angle between the planes being 12.9(2)° and 25.6(4)° in **4** and **2**, respectively. Scanning through the torsion angles along the *ansa*-chain, one observes an interesting feature: the torsion angles N(1)–C(15)–C(16)–C(17) and C(15)–C(16)–C(17)–C(18) in **4** have values of 62.5(4)°

Table 4. *Distances* [Å] *between O(1), O(2), O(9), and O(10) in* **2** [11] *and* **4**. Standard deviations in parentheses.

	2	**4**		**2**	**4**
O(1)–O(2)	2.557 (6)	2.572 (3)	O(2)–O(9)	9.208 (6)	8.088 (3)
O(1)–O(9)	8.384 (6)	7.437 (3)	O(2)–O(10)	9.004 (7)	7.579 (4)
O(1)–O(10)	7.545 (7)	6.207 (4)	O(9)–O(10)	2.632 (7)	2.687 (5)

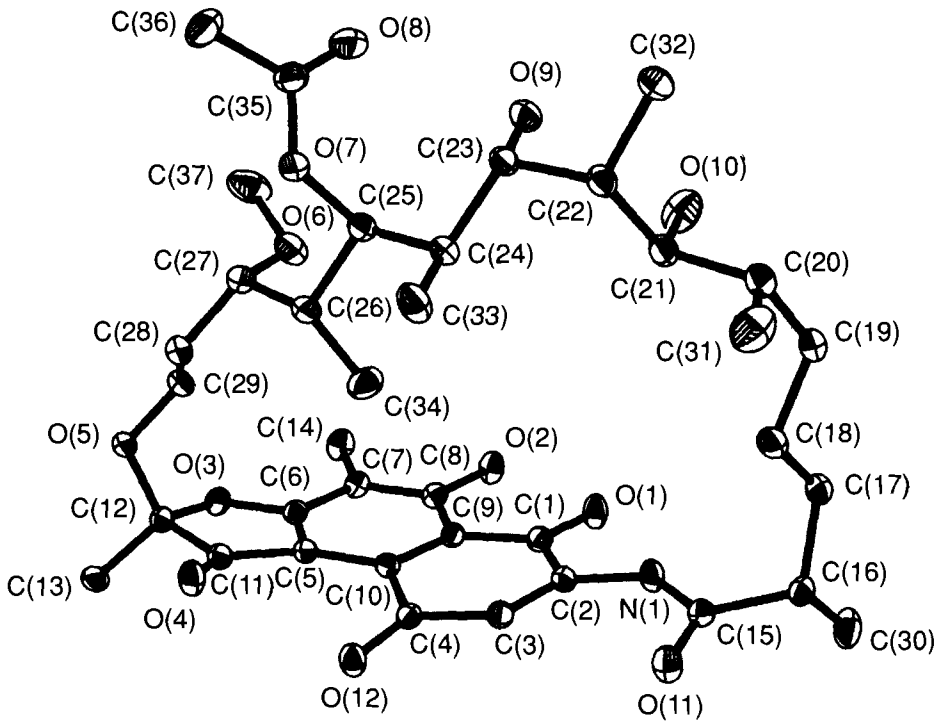

Fig. 1. *A perspective view of molecule* **4**. Thermal ellipsoids are drawn at 20% probability level.

Table 5. *Torsion Angles* [°] *along the Skeleton of the* ansa-*Chain of* **2** [11] *and* **4**. Standard deviations in parentheses.

	2	**4**		**2**	**4**
C(1)–C(2)–N(1)–C(15)	166.2 (5)	–176.2 (3)	C(21)–C(22)–C(23)–C(24)	64.9 (5)	57.5 (4)
C(2)–N(1)–C(15)–C(16)	–163.4 (5)	–173.8 (3)	C(22)–C(23)–C(24)–C(25)	–168.4 (4)	–172.1 (3)
N(1)–C(15)–C(16)–C(17)	132.9 (6)	62.5 (4)	C(23)–C(24)–C(25)–C(26)	172.1 (4)	176.7 (3)
C(15)–C(16)–C(17)–C(18)	–3.5 (9)	51.8 (4)	C(24)–C(25)–C(26)–C(27)	–164.6 (4)	–172.6 (3)
C(16)–C(17)–C(18)–C(19)	–173.5 (6)	164.9 (3)	C(25)–C(26)–C(27)–C(28)	–165.0 (4)	–171.4 (3)
C(17)–C(18)–C(19)–C(20)	176.2 (5)	172.9 (3)	C(26)–C(27)–C(28)–C(29)	–113.7 (6)	–115.3 (4)
C(18)–C(19)–C(20)–C(21)	–60.7 (7)	–71.7 (4)	C(27)–C(28)–C(29)–O(5)	–179.6 (5)	–179.0 (3)
C(19)–C(20)–C(21)–C(22)	–177.3 (4)	–178.3 (3)	C(28)–C(29)–O(5)–C(12)	–134.7 (5)	–117.6 (3)
C(20)–C(21)–C(22)–C(23)	–170.2 (4)	–175.5 (3)	C(29)–O(5)–C(12)–O(3)	–65.0 (5)	–59.2 (3)

and 51.8(4)°, respectively, while in **2** the values are 132.9(6) and −3.5(9)°, respectively (*Table 5*). It is worthy of note that hydrogenation results in a local rearrangement of the N(1)–C(18) region, whereas the conformation of the remaining part of the *ansa*-chain is very much the same as that observed in **2** and in several related active rifamycins [12].

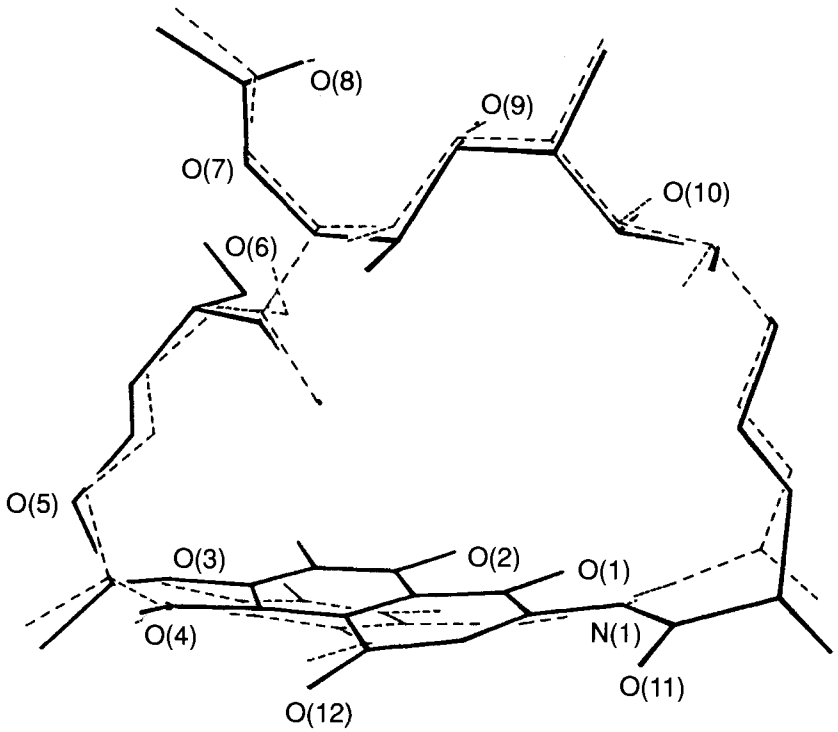

Fig. 2. *A perspective view of molecules* **2** (broken line) *and* **4** (full line) *superimposed*

Activity Measurements. – The tetrahydro-, hexahydro-, and 3-substituted tetrahydrorifamycins S **3**–**10** were tested as inhibitors of bacterial DDRP with respect to **2** and to 18,19-dihydrorifamycin S [5], in order to define the structure-activity relationship as a function both of the extent of hydrogenation and of the chirality at C(16). It was found that hydrogenation of the double bonds proportionally reduces activity. The (16*R*)-epimers are more active than the (16*S*)-epimers (*Table 6*).

Table 6. *Inhibitory Power as* IC_{50} [μM] *of Hydrogenated Rifamycins on DDRP from* E. coli (1 unit), *Determined as Described in* [10]

	IC_{50} [μM]		IC_{50} [μM]
Rifamycin S (**2**)	0.05	(16*R*)-16,17,18,19,28,29-Hexahydro-	7
18,19-Dihydrorifamycin S[a])	0.15	rifamycin S (**5**)	
(16*R*)-3-Bromo-16,17,18,19-tetrahydro-	0.50	(16*R*)-16,17,18,19-Tetrahydro-	16
rifamycin S (**7**)		3-(piperidin-1-yl)rifamycin S (**9**)	
(16*R*)-16,17,18,19-Tetrahydrorifamycin S (**3**)	1.3	(16*S*)-16,17,18,19-Tetrahydro-	26
(16*S*)-3-Bromo-16,17,18,19-tetrahydro-	1.6	3-(piperidin-1-yl)rifamycin S (**10**)	
rifamycin S (**8**)		(16*S*)-16,17,18,19,28,29-Hexahydro-	> 30
(16*S*)-16,17,18,19-Tetrahydrorifamycin S (**4**)	1.6	rifamycin S (**6**)	

[a]) Data from [5].

The structural study of **4** indicates that the four atoms O(1), O(2), O(9), and O(10) are differently located in hydrogenated derivatives with respect to their position in **2** and in other rifamycins active on wild-type DDRP [12]. The activity of compounds **7**–**10** was also tested on *Rif*-resistant DDRP, to verify if such displacement of the groups responsible for the main inhibiting interaction with the wild-type enzyme could by chance restore to some extent such an interaction with the *Rif*-resistant enzyme. No activity was found in those compounds up to a concentration of 10 μM.

Conclusions. – The lower activity shown by **4** with respect to **2** can be tentatively explained on the basis of a higher flexibility of the *ansa*-chain which causes the closing of the angle between the chromophore rings and the *ansa*-chain plane by 18.7°. A significant shortening (average 1.14 Å) in the cross-distances O(1)–O(9), O(1)–O(10), O(2)–O(9), and O(2)–O(10) is observed in **4** if compared with those in **2** (*Table 4*), while the C(16) to O(5) fragment of the *ansa*-chain has the same conformation in **4** as in **2** (*Table 5*). It is suggested that the pattern of these four O-atoms, supposed to play a key-role in the inhibitory interaction of these antibiotics with the bacterial enzyme [1] [10] is in **4** and in general in tetrahydrorifamycin-S derivatives 'well-oriented', but not 'well-positioned'. An additional effect seems to be due to the chirality at C(16), and therefore, to the position of Me(30). It is not possible to understand whether this is due to a sterically induced conformational effect on the *ansa*-chain, or to some direct hydrophobic interaction by the Me group itself.

The differences in activity within epimeric pairs are more evident in derivatives of **3** and **4** in which either activating (see **7** and **8**) or deactivating groups (see **9** and **10**) [10] have been introduced at C(3) (*Table 6*). The hydrogenation of all three double bonds, as in **5** and **6**, most probably causes an even more pronounced displacement of the position of O(1), O(2), O(9), and O(10), so that hexahydrorifamycins are much less active than tetrahydrorifamycins.

The authors wish to thank the NMR, microanalysis, and graphic services of the CNR, Area della Ricerca di Roma.

Experimental Part

1. *General.* TLC: glass plates, silica gel *60* F_{254} (0.25 mm) *Merck*. Prep. TLC: glass plates, silica gel *60* (2 mm) *Merck*. Column chromatography (CC): silica gel *60* (0.063–0.200 mm) *Merck*, acid-washed [3] and deactivated with 10% H_2O (*v/w*). UV Spectra: *Varian DMS90*, in 40 mM *Tris*-HCl, pH 7.8, DMSO 1%. NMR Spectra: *Varian-XL-300* spectrometer, 300 MHz for ^1H for **7**–**10**; *Bruker-AMX* spectrometer, 600.13 MHz for ^1H and 150.9 MHz for ^{13}C for **3**–**6**; in $CDCl_3$; chemical shifts in ppm rel. to Me_4Si (=0 ppm); partial ^1H-assignment (CH, CH_3) by 2D-DQ-filtered COSY [13]; ^{13}C-spectra were run WALTZ-decoupled [14]; CH_2's were distinguished through DEPT editing [15]; ^1H,^{13}C 2D heteronuclear correlation maps were obtained by reverse detection [16]; assignment of methylenes by comparison of hetero-correlated and COSY maps. FAB-MS: *Kratos MS-80*; samples in ethyleneglycol in the presence of CsI. Elemental analysis for C,H,N was in agreement with calculated values within ±0.5%.

2. *(16R)- and (16S)-16,17,18,19-Tetrahydrorifamycin S* (**3** and **4**, resp.). Rifamycin S (= *1,4-dideoxy-1,4-dihydro-1,4-dioxorifamycin*; **2**; 500 mg) was hydrogenated over Pd/C in EtOH as described in [2]. After filtration over *Celite* and evaporation, the solid residue was submitted to CC ($CHCl_3$/MeOH 4:1) giving 2 main fractions. TLC ($CHCl_3$/MeOH 9:1): R_f 0.5 and 0.1. By oxidation with $K_3[Fe(CN)_6]$, the former gave **4** (360 mg, 72%) and the latter **3** (100 mg, 20%).

(16R)-Epimer **3**. UV: 308 (4.16), 527 (3.48). ^1H-NMR: *Table 1*. ^{13}C-NMR: *Table 2*. FAB-MS: 832 ($[M + 1 + Cs]^+$).

(16S)-Epimer **4**. UV: same as **3**. ^1H-NMR: *Table 1*. ^{13}C-NMR: *Table 2*. FAB-MS: 832 ($[M + 1 + Cs]^+$).

3. *(16R)- and (16S)-16,17,18,19,28,29-Hexahydrorifamycin S* (**5** and **6**, resp.). Rifamycin S (**2**; 300 mg), or **3** (160 mg), or **4** (100 mg) was hydrogenated over PtO_2 in EtOH as described in [2] [3]. After filtration over *Celite* and evaporation, the residues were purified by CC ($CHCl_3$/MeOH 80:20). After purification, each compound was oxidized with $K_3[Fe(CN)_6]$. The products derived from **3** and **4** were pure **5** and **6**, resp.; **2** gave a mixture of two products which, after separation and oxidation as described above, proved to be pure **5** and **6** in a ratio 1:3.7. (Overall yield of hydrogenation over PtO_2: 60%.) TLC: R_f of hydroquinone form of **5** and **6** identical to those of **3** and **4**, resp.

(16R)-Epimer **5**. UV: 309 (4.16), 521 (3.45). ^{1}H-NMR: *Table 1*. ^{13}C-NMR: *Table 2*.

(16S)-Epimer **6**. UV: same as **5**. ^{1}H-NMR: *Table 1*. ^{13}C-NMR: *Table 2*.

4. *(16R)- and (16S)-3-Bromo-16,17,18,19-tetrahydrorifamycin S* (**7** and **8**, resp.). Rifamycin SV (**1**; 500 mg), was brominated at C(3), as described in [8], to give, after workup, oxidation, and purification by CC, 3-bromorifamycin S (100 mg, 18%). This was dissolved in 95% EtOH (7.5 ml) and added to a suspension of Rh/Al_2O_3 (30 mg) in 95% EtOH (3 ml) pre-saturated with H_2. After 4 h stirring at r.t. and atmospheric pressure, the mixture was filtered through *Celite*, evaporated, oxidized with $K_3[Fe(CN)_6]$, and purified by CC (10 g of silica gel, benzene/AcOEt 3:2): **7** (5 mg, 5%) and **8** (10 mg, 10%).

By bromination of the hydroquinone-SV form of **3** and **4**, under the same conditions as above, we obtained **7** (yield 15%) and **8** (yield 20%), resp.

(16R)-Epimer **7**. UV: 311 (4.20), 430 (3.39), 530 (3.55). ^{1}H-NMR: *Table 3*.

(16S)-Epimer **8**. UV: same as **7**. ^{1}H-NMR: *Table 3*.

5. *(16R)- and (16S)-16,17,18,19-Tetrahydro-3-(piperidin-1-yl)rifamycin S* (**9** and **10**, resp.). Rifamycin S (**2**, 1 g) was reacted with piperidine as described in [4] to give, after workup, oxidation, and purification by CC, 830 mg (75%) of 3-(piperidin-1-yl)rifamycin S. This (500 mg) was hydrogenated over Pd/C as indicated above, oxidized to the quinone-S form with an equivalent (*w*/*w*) amount of MnO_2 in MeCN, and purified by prep. TLC (benzene/AcOEt 2:3): **9** (55 mg, 11%) and **10** (65 mg, 13%).

By reaction of **3** and **4** with piperidine, under the same conditions as above, we obtained **9** (yield 80%) and **10** (yield 80%), resp.

(16R)-Epimer **9**. UV: 307 (4.18), 453 (3.50). ^{1}H-NMR: *Table 3*.

(16S)-Epimer **10**. UV: same as **9**. ^{1}H-NMR: *Table 3*.

6. *X-Ray Analysis of* **4**. Orange prismatic crystals were grown from MeOH/H_2O at 277 K. Crystal data: $C_{37}H_{49}NO_{12}\cdot$MeOH, $M_r = 731.8$; space group monoclinic $P2_1$; $a = 10.247(2)$, $b = 9.648(2)$, $c = 19.800(3)$ Å; $\beta = 97.11(2)°$; $V = 1942.4(6)$ Å^3; $F(000) = 784$, $Z = 2$, $D_x = 1.251$ g·cm^{-3}, CuK_α, $\lambda = 1.54184$ Å, $\mu = 7.80$ cm^{-1}. A crystal of dimensions 0.5 × 0.3 × 0.2 mm was used for data collection and set on a *Siemens R3m/V* diffractometer (graphite-monochromated CuK_α radiation). Intensity data were collected, the exper. conditions being: $(\sin\Theta/\lambda)_{max} = 0.61$ Å^{-1}, 2Θ–Θ scan mode, scan width $(2 + 0.15\tan\Theta)°$, scan rate 1.00–14.65°·min^{-1} (depending on reflection intensity), background-count time half of the total scan time. Accurate unit-cell parameters were determined by least-squares fit of the setting angles of 20 selected reflections with $66 \leqslant 2\Theta \leqslant 80°$. There was no significant intensity variation for the three check reflections −1, −2,1, −1, −1,0, and −1,0,3, monitored every hundred. The data were corrected for *Lorentz* and polarization effects, but no absorption or extinction corrections were made. Of the 4287 unique reflections measured ($R_{int} = 2.42\%$), 3900 with $F_o \geqslant 8.0\sigma(F_o)$ were considered as observed. The structure was solved by direct methods using the SHELXTL-Plus [17] program based on the multiple-permutation single-solution procedure, and refined on F_o by full-matrix least-squares methods (number of refined parameters was 468 and the data to parameter ratio 8.3:1). Difference *Fourier* syntheses, computed at the end of the anisotropic least-squares refinement, showed all H-atoms in configurationally feasible positions. Those of the MeOH molecule were not included in the refinement. The final refinements were carried out by full-matrix with H-atoms allowed to ride on the corresponding C-, N-, and O-atoms with isotropic temperature factors $U_{iso} = 0.08$ Å^2. The final R value was 0.048 and $R_w = 0.069$ minimizing the function $w|\Delta F|^2$, with $w = [\sigma^2(F_o) + 0.0034F_o^2]^{-1}$. At convergence, the maximum shift/e.s.d. ratio was less than 0.02 and $S = 1.14$. Heights in final difference *Fourier* map $\rho_{max} = 0.36$, $\rho_{min} = -0.26$ e·Å^{-3}. Atomic scattering factors were taken from [18]. Final positional and equivalent isotropic thermal parameters U_{eq} were deposited with the *Cambridge Crystallographic Data Centre*. The PARST program [19] was used for the molecular-geometry calculations.

7. *Activity Measurements*. The inhibitory activity of **2**–**10** and of 18,19-dihydrorifamycin S was measured on 1 unit of DDRP from *E. coli* (*Boehringer*, Mannheim) and on 1 unit of *Rif*-resistant DDRP from *Rif*-resistant *E. coli* (*Promega*, Madison), according to standard procedures [10]. Approximate IC_{50} values were first extrapolated from plots of the percent of inhibition *vs.* the log of the inhibition concentration, for concentrations in the

range 0.01–10 μM. Each exper. point of the curves was calculated as the mean value of four determinations, the average relative error being *ca.* ±10%. The IC_{50} values reported in *Table 6* were then measured by running inhibition experiments at inhibitor concentrations ranging within ±30% of the extrapolated value.

REFERENCES

[1] M. Brufani, 'The Ansamycins', in 'Topics in Antibiotic Chemistry', Ed. P. G. Sammes, Ellis Horwood Ltd., Chichester, 1977, Vol. 1, pp. 91–212; G. Lancini, W. Zanichelli, 'Structure-Activity Relationships in Rifamycins', in 'Structure-Activity Relationships among the Semisynthetic Antibiotics', Ed. D. Perlman, Academic Press, New York, 1977, pp. 531–596.
[2] W. Oppolzer, V. Prelog, P. Sensi, *Experientia* **1964,** *20,* 336.
[3] W. Kump, H. Bickel, *Helv. Chim. Acta* **1973,** *56,* 2323.
[4] W. Kump, H. Bickel, *Helv. Chim. Acta* **1973,** *56,* 2348.
[5] A. D. Bianco, M. Brufani, D. Capitani, L. Cellai, M. Guiso, C. Rossi, A. L. Segre, *Gazz. Chim. Ital.* **1989,** *119,* 585.
[6] P. Traxler, Th. Schupp, W. Wehrli, *J. Antibiot.* **1982,** *35,* 594.
[7] W. Wehrli, M. Staehelin, *Biochim. Biophys. Acta* **1969,** *182,* 24.
[8] M. F. Dampier, C. W. Chen, H. W. Whitlock *J. Am. Chem. Soc.* **1976,** *98,* 7064.
[9] J. Leitich, W. Oppolzer, V. Prelog, *Experientia* **1964,** *20,* 343.
[10] L. Cellai, H. Heumann, G. Baer, *Eur. J. Med. Chem.* **1989,** *24,* 105.
[11] S. K. Arora, *J. Med. Chem.* **1985,** *28,* 1099.
[12] S. Cerrini, D. Lamba, M. C. Burla, G. Polidori, A. Nunzi, *Acta Crystallogr., Sect. C* **1988,** *44,* 489.
[13] A. J. Shaka, R. Freeman, *J. Magn. Reson.* **1983,** *51,* 169.
[14] A. J. Shaka, J. Keeler, R. Freeman, *J. Magn. Reson.* **1983,** *53,* 313.
[15] O. W. Sørensen, R. R. Ernst, *J. Magn. Reson.* **1983,** *51,* 477.
[16] A. Bax, R. H. Griffy, B. L. Hawkins, *J. Magn. Reson.* **1983,** *55,* 301.
[17] G. M. Sheldrick, 'SHELXTL Plus Release 4.1 for *Siemens R3m/V* Crystallographic Research Systems', *Siemens Analytical X-Ray Instruments, Inc.,* Madison, Wiscon., USA, 1990.
[18] 'International Tables for X-Ray Crystallography', Kynoch Press, Birmingham (present distributor, Kluwer Academic Publishers, Dordrecht), 1974, Vol. IV.
[19] M. Nardelli, *Comput. Chem.* **1983,** *7,* 95.